

CHAPTER - V

PREPARATION AND CHARACTERISATION OF Sb_2Se_3 THIN FILMS FROM AQUEOUS MEDIUM

5.1	INTRODUCTION	93
5.2	EXPERIMENTAL	94
5.2.1	Thin film deposition	94
5.2.1.1	Film preparation using SeO_2	94
5.2.1.2	Annealing of Sb_2Se_3 thin films	96
5.2.1.3	Film preparation using $\text{CSe}(\text{NH}_2)_2$	96
5.2.2	CHARACTERIZATION OF Sb_2Se_3 THIN FILMS	97
5.2.2.1	X-ray diffraction (XRD)	97
5.2.2.2	Scanning electron microscopy (SEM)	97
5.2.2.3	Optical absorption	97
5.2.2.4	Electrical resistivity	97
5.2.2.5	Thermoelectric power (TEP)	97
5.3	RESULTS AND DISCUSSION	98
5.3.1	X-ray diffraction (XRD)	98
5.3.2	Scanning electron microscopy (SEM)	100
5.3.3	Optical absorption	102
5.3.4	Electrical resistivity	104
5.3.5	Thermoelectric power (TEP)	106
5.3.6	Annealing of Sb_2Se_3 thin films	108
	REFERENCES	109

5.1 INTRODUCTION

The search for new materials to satisfy the practical demand and the use of electronic and optical devices has stimulated considerable interest in the growth and understanding of semiconductor properties of metal chalcogenides. Antimony triselenide is a layer structured semiconductor of orthorhombic crystal structure. The studies of amorphous films of Sb-Se system have been attracting wide attention in the last few decades due to its good photovoltaic properties and high thermoelectric power which allow possible applications for optical and thermoelectric cooling devices..

The optical absorption coefficient at photon energies from 1.15 to 1.7 eV and photoconductive spectral responses at 1-24 eV have been measured [1-7] for single crystals and amorphous films of Sb_2Se_3 . The reported values for the indirect forbidden gap are 1.34 eV and 1.14 eV for the amorphous and crystalline films respectively. An empirical relation was proposed by Shimakawa [8] and Tichy [9] to interpret the compositional dependence of the optical gap in amorphous semiconducting alloys. The effect of a systematic variation of x in $\text{Sb}_x\text{Se}_{1-x}$ thin films on its optical properties has been studied [10 -12].

In the present chapter emphasis is given on the deposition of Sb_2Se_3 thin films from aqueous medium using two different Se sources and study of their structural, optical and electrical properties.

5.2 EXPERIMENTAL

Sb₂Se₃ thin films have been deposited by the spray pyrolysis technique as discussed in section 3.2.1.1.

5.2.1 Thin film deposition

Substrate cleaning

The substrate cleaning procedure discussed in section 3.2.1.2 is used to clean the glass substrates.

5.2.1.1 Film preparation using SeO₂

Freshly prepared deionised double distilled water is used to prepare the solutions. Initial ingredients used for the deposition of Sb₂Se₃ films are as follows:

1. A.R. Grade antimony trichloride [SbCl₃] supplied by s.d. fine Chem. Ltd., Boisar - 401 501.
2. A.R. Grade hydrochloric acid [HCl], supplied by Qualigens fine Chemicals, Mumbai.
3. A.R. Grade tartaric acid [C₄H₆O₆] supplied by Loba Chemie Industrial Company, Mumbai.
4. A.R. Grade selenium dioxide [SeO₂] supplied by Qualigens fine Chemicals, Mumbai.

Solution of SbCl₃ was prepared as discussed in section 3.2.1.3.

Sb₂Se₃ thin films were deposited by spraying a tartaric acid complex of SbCl₃ and SeO₂ in appropriate volumes to obtain Sb:Se ratio as 2:3. The spray rate was kept constant at 3 cc min⁻¹. 10 cc of tartaric acid was mixed with 8 cc

of SbCl_3 . Then 12 cc of SeO_2 solution was added into complexed SbCl_3 and immediately sprayed onto hot glass substrates maintained at desired substrate temperature. When the droplets of the sprayed solution reach the hot substrates, owing to pyrolytic decomposition of the solution, uniform, pinhole free, brown coloured and well adhesive films of Sb_2Se_3 are formed on the substrates. The films are allowed to cool to room temperature and are taken out of the deposition chamber to preserve them in dark dessicator.

Spray rate

The spray rate can be varied by changing the air pressure of the carrier gas or height of the liquid level monitor as discussed in section 3.2.1.5. During the Sb_2Se_3 film deposition the spray rate was maintained to be 3 cc min^{-1} .

Substrate temperature

To optimize the substrate temperature, equimolar (0.1 M) solution of SbCl_3 and SeO_2 was sprayed with spray rate of 3 cc min^{-1} . The concentration of complexing agent was kept constant at 0.5 M. The films were deposited on to the set of glass substrates, in different sets, maintained at temperatures of 275, 300, 325 and 350 $^\circ\text{C}$. The structural and electrical analysis of these films reveals that the films prepared at 300 $^\circ\text{C}$ have relatively higher conductivity as compared to the films deposited at other substrate temperatures. Thus 300 $^\circ\text{C}$ is considered as the optimised substrate temperature [13].

Concentration of spraying solution and complexing agent

Concentration of spraying solution and complexing agent was optimised to be 0.1 and 0.5M respectively as per the procedure discussed in sections 3.2.1.7 and 3.2.1.8.

5.2.1.2 Annealing of Sb_2Se_3 thin films

The annealing of Sb_2Se_3 thin films is carried out using high temperature tubular furnace supplied by Tours and Associates, Adyar, Madras in nitrogen atmosphere at temperature of 325°C for 2 hours.

5.2.1.3 Film preparation using $CSe(NH_2)_2$

Sb_2Se_3 thin films were deposited by spraying a tartaric acid complex of aqueous $SbCl_3$ and selenourea [$CSe(NH_2)_2$] solutions in appropriate volumes in order to obtain Sb:Se ratio as 2:3. The substrate temperature, the concentration of solution and concentration of complexing agent (tartaric acid) were optimised, as discussed in sections 3.2.1.6 to 3.2.1.8, as 275 °C 0.01 M and 0.5M respectively. The spray rate was kept constant at 5 cc min⁻¹. 10 cc solution of tartaric acid was mixed with 5 cc of 0.01 M antimony trichloride. Then 12 cc of 0.01 M selenourea was added into the complexed $SbCl_3$ and immediately sprayed onto the hot glass substrates maintained at temperature of 275°C. The films were bluish brown in colour, uniform, pinhole free and well adherent to the glass substrates.

5.2.2 CHARACTERISATION OF Sb_2Se_3 THIN FILMS

The Sb_2Se_3 films prepared using two different Se sources and at optimised preparative parameters were characterized by using X-ray diffraction, scanning electron microscopy, optical absorption, dark resistivity and TEP measurement techniques.

5.2.2.1 X- ray diffraction (XRD)

XRD studies were carried out as discussed in section 3.2.2.1.

5.2.2.2 Scanning electron microscopy (SEM)

SEM studies were carried out as discussed in section 3.2.2.2.

5.2.2.3 Optical absorption

To carry out the optical absorption studies the procedure discussed in section 3.2.2.3 was adopted.

5.2.2.4 Electrical Resistivity

To study the electrical characterisation of the films, dark resistivity measurements were carried out using two point d.c. probe method in the temperature range 300 to 500K. The details of experimental setup are discussed in Section 3.2.2.4.

5.2.2.5 Thermoelectric power (TEP)

The details of the experimental setup of TEP are given in section 3.2.2.5.

5.3 RESULTS AND DISCUSSION

The thickness of the prepared films was determined using relation 2.1 by weight difference method. The density of the deposited material is taken to be 5.81 gm / cm^3 . The thickness of the Sb_2Se_3 films deposited using SeO_2 and $\text{CSe}(\text{NH}_2)_2$ as Se sources were found to be $0.46 \text{ }\mu\text{m}$ and $0.51 \text{ }\mu\text{m}$ respectively.

5.3.1 X-ray diffraction (XRD)

XRD patterns of Sb_2Se_3 thin films prepared using two different Se sources are studied in order to reveal their structures.

Films using SeO_2

The appearance of the broad X- ray spectrum (Fig. 5.1) for the films suggests that the material formed is amorphous.

Films using $\text{CSe}(\text{NH}_2)_2$

Fig. 5.1 also shows the XRD pattern for the Sb_2Se_3 film prepared using $\text{CSe}(\text{NH}_2)_2$ as a Se source. It has been found that the films are polycrystalline with orthorhombic crystal structure. The comparison of American Standards and Testing Materials (ASTM) data [14] of Sb_2Se_3 with the observed d values confirms the formation of Sb_2Se_3 material. Table 1 shows comparison of the observed and standard d values for the deposited films.

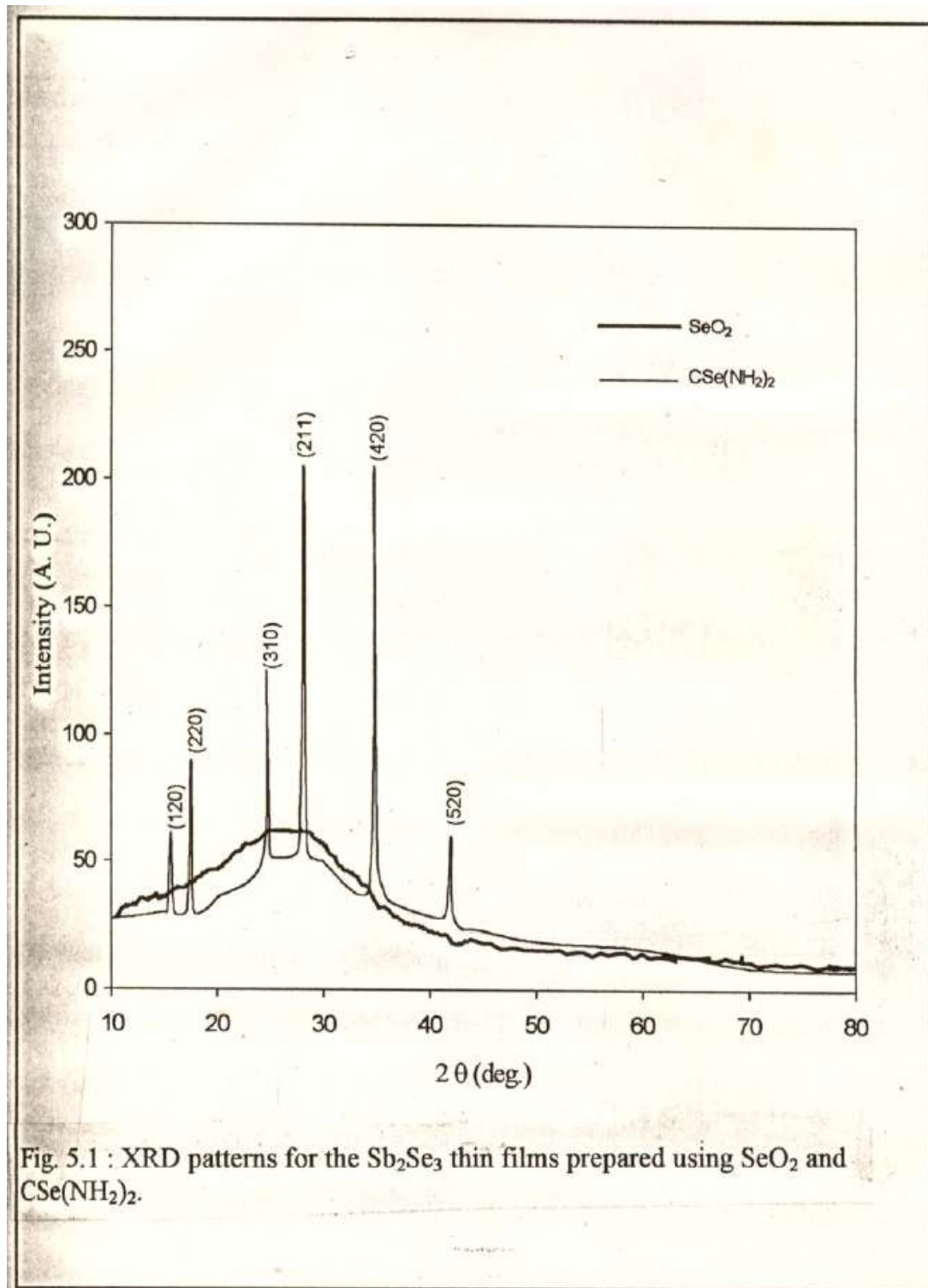


Table 1 : Comparison of the observed d values of Sb_2Se_3 thin films with standard ASTM data.

Standard d values (Å)	Observed d values (Å)	I/Imax (%)	(hkl) planes
5.25	5.2508	76.70	(120)
4.14	4.1235	60.28	(220)
3.682	3.6730	40.93	(310)
3.162	3.1713	100.00	(211)
2.608	2.5981	100.00	(420)
2.164	2.1500	21.13	(520)

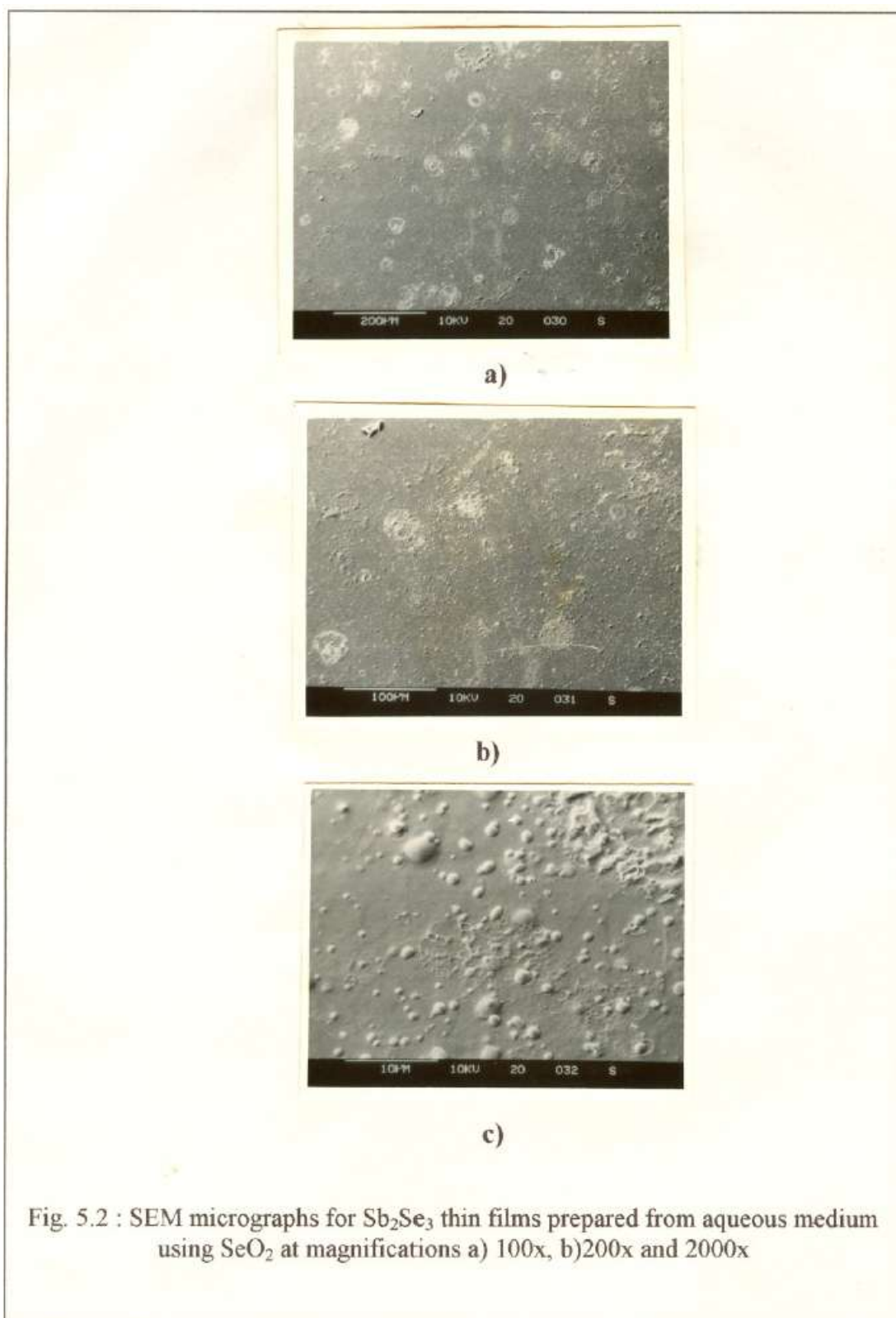
The calculated lattice constants are found to be $a = 12.1817 \text{ \AA}$; $b = 11.2906 \text{ \AA}$ and $c = 4.0384 \text{ \AA}$ [16] which are close to the values reported for single crystals of Sb_2Se_3 [2,15].

The structural difference between the Sb_2Se_3 films prepared using SeO_2 and $\text{CSe}(\text{NH}_2)_2$ as Se sources is owing to the difference in stoichiometric proportion, certainly due to different reaction mechanisms occurring, during pyrolytic decomposition of the Sb_2Se_3 particles.

5.3.2 Scanning electron microscopy (SEM)

Films using SeO_2

The SEM images at various magnifications are shown in Fig. 5.2 (a- c). The films are continuous with fine grains. The film surface is rough and shows the presence of overgrown particles.



Films using CSe(NH₂)₂

SEM Micrographs of thin films deposited using CSe(NH₂)₂ as a Se source are shown in Fig. 5.3 for three different magnifications. The micrograph at 5000x magnification [Fig. 5.3 (a)] shows total coverage of the substrate by the film with rough surface. Fig. 5.3 (b) and (c) shows micrograph of the same film at magnifications 10000x and 20000x respectively. It shows random distribution of overgrowth of particles.

Difference in observed surface topography of the films prepared using two Se sources is due to the difference in the film structure for two films.

5.3.3. Optical absorption

Films using SeO₂

The variation of optical density (αt) with wavelength (λ) for the Sb₂Se₃ films is shown in Fig. 5.4. α is found to be of the order of 10⁴ cm⁻¹. Following the theoretical analysis, the energy dependence of absorption coefficient can be expressed by the relation 2.8 for amorphous semiconductors [3-10] with $n = 2$.

The absorption of photon energy for amorphous Sb₂Se₃ films has been explained by many workers [1-7, 10]. Fig. 5.5 shows the plot of $(\alpha h\nu)^{1/2}$ versus $h\nu$. The optical gap, obtained by extrapolating the straight line portion of the plot at $\alpha = 0$, is found to be 1.28 eV. This value is very close to the value of optical gap reported for single source evaporated film of Sb₂Se₃ [3].



a)



b)



c)

Fig. 5.3 : SEM micrographs for Sb₂Se₃ thin films prepared from aqueous medium using CSe(NH₂)₂ at magnifications a) 5000x, b)10000x and 20000x

Films using CSe(NH₂)₂

The variation of optical density (α) with wavelength (λ) is shown in Fig. 5.4. α is of the order of 10^4 - 10^5 cm⁻¹. The energy dependence of absorption coefficient on energy of photon ($h\nu$) can be expressed by the relation 2.8 for allowed direct transition with $n = 1/2$.

Optical gap, due to direct transition of 1.21 eV for single crystals of Sb₂Se₃ has already been reported [3]. In the present investigation the measurements are carried out at room temperature where the absorption will be due to a band to band transition as the excitation band is not likely to be present. This is confirmed by plotting $(\alpha h\nu)^2$ versus $h\nu$ as shown in Fig. 5.5. The plot is straight line indicating that the direct transition is dominant transition involved. Extrapolation of the linear portion of the plot to energy axis at $\alpha = 0$ gives the optical gap of 1.26 eV. The deduced value is very near to the literature value for Sb₂Se₃ single crystal [3].

The values of the energy band gap for the amorphous and polycrystalline Sb₂Se₃ are close considering that the short range order in the two phases are identical [17].

5.3.4 Electrical resistivity

Two point d.c. dark resistivity measurements show that the Sb₂Se₃ films prepared using SeO₂ as well as CSe(NH₂)₂ as a Se source are highly resistive. The room temperature dark resistivity for both the films is of the order of 10^6 - 10^7 Ω .cm similar to the results of others [18]. The high resistivity of the film

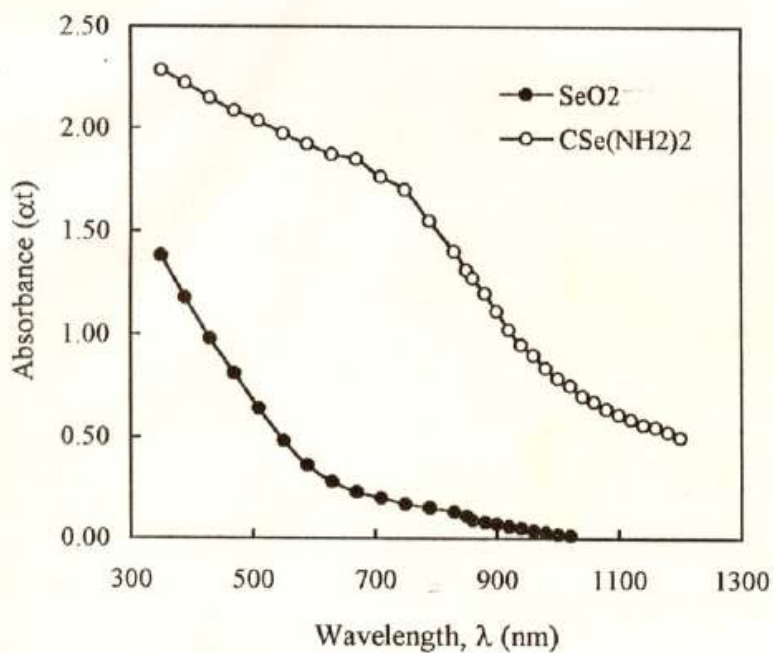


Fig. 5.4 : Variation of optical absorbance (αt) with wavelength (λ) for sprayed Sb_2Se_3 films prepared using two Se sources.

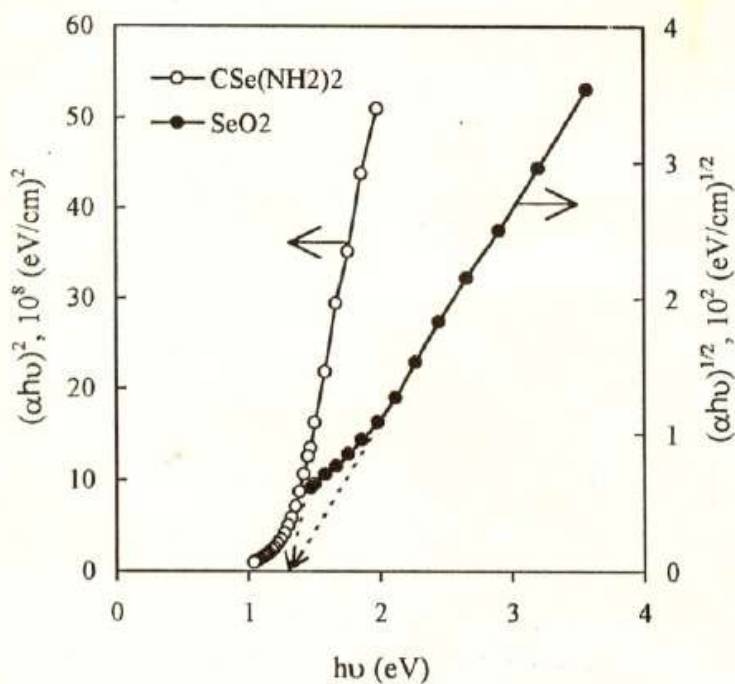


Fig. 5.5 : Plot of $(\alpha h\nu)^{1/2}$ and $(\alpha h\nu)^2$ vs. $h\nu$ for the Sb_2Se_3 films prepared using SeO_2 and $\text{CSe}(\text{NH}_2)_2$ respectively.

may be due to discontinuities, large grain boundaries and low thickness of the film.

Films using SeO₂

The variation of $\log(\rho)$ with reciprocal of temperature is depicted in Fig. 5.6. It has been seen that the resistivity decreases with increase in temperature and supports for the semiconducting nature of the Sb₂Se₃ films. The calculated activation energy for the films is observed to be 0.74 eV.

Films using CSe(NH₂)₂

The variation of $\log(\rho)$ with $1000/T$ for Sb₂Se₃ films deposited using CSe(NH₂)₂ is depicted in Fig. 5.6. The electrical resistivity and thermal activation energy have been estimated using relation 2.4 for resistivity. From the slope of $\log(\rho)$ versus $1000/T$ plot, the value of activation energy was calculated. The observed activation energy for the film is 0.77 eV.

The observed activation energy for both the films is nearly same which may be attributed to the identical short range orders for both the films [17].

5.3.5 Thermoelectric power (TEP)

The thermoelectric power measurements were used to determine the type of the charge carriers of the material being studied.

Films using SeO₂

Figure 5.7 shows the generated thermoelectric e.m.f. for the films within the temperature difference of 0 - 100 °C. It shows that the e.m.f. varies linearly with temperature difference, thus TEP does not vary with temperature.

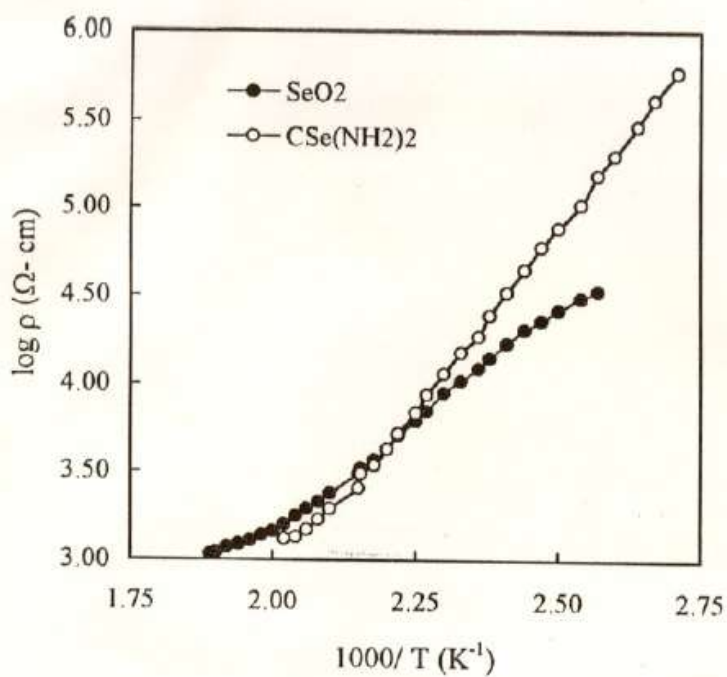


Fig. 5.6 : Plot of $\log \rho$ against $1000/T$ for Sb_2Se_3 films prepared using two Se sources.

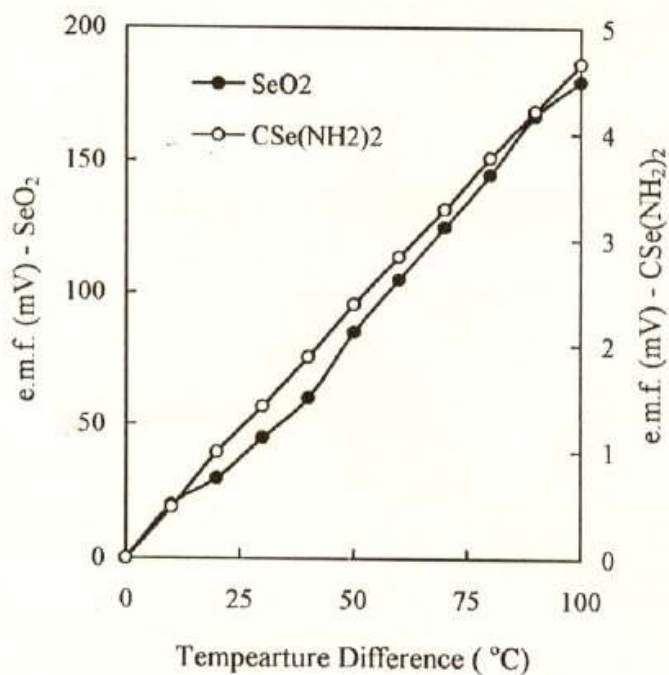


Fig. 5.7 : Thermo emf versus temperature difference for Sb_2Se_3 films prepared using two Se sources.

Positive polarity of the generated thermoelectric voltage has been found, which suggests that the conduction in both the films has been of p-type [13,19]. The observed value of thermoelectric power (TEP) is of the order of $1 \text{ mV}/^\circ\text{C}$.

Films using $\text{CSe}(\text{NH}_2)_2$

The variation of generated thermo e.m.f. with temperature difference (0 - 100°C) has been depicted in Fig. 5.7. The films prepared using $\text{CSe}(\text{NH}_2)_2$ source have shown p-type conductivity [16,19]. The observed TEP is $46\mu\text{V}/^\circ\text{C}$.

5.3.6 Annealing of Sb_2Se_3 thin films

Sb_2Se_3 films prepared using SeO_2 and $\text{CSe}(\text{NH}_2)_2$ were annealed in N_2 atmosphere at 325°C for 2 hours to see its effect on crystallinity of the films. It is observed that the annealing has no effect on the crystallinity of the films.

REFERENCES

1. C. Wood, Z. Harych and J.C. Shaffer, *J. Non-Cryst. Solids*, 8 - 10 (1972) 209.
2. J.C. Shaffer, B. Von Pelt, C. Wood, J. Freeouf, K. Murase and J.W. Osman, *phys. status solidi (b)*, 54 (1972) 511.
3. C. Wood, L.R. Gilbert, V. Van Pelt. and Wolffing, *phys. status solidi (b)*, 68 (1975) K39.
4. T. Fujita, K. Kurita, K. Takiyama and T. Oda, *J. Lumin.*, 39 (1998) 175.
5. T. Fujita, K. Kurita, K. Takiyama and T. Oda, *J. Phys. Soc. Japn.*, 56 (1987) 3737.
6. H.S. Soliman, W.Z. Soliman, M.M. El - Nahas and Kh.A. Mady, *Optica Pura Y Aplicada*, 22 (1989) 115.
7. K. Shimakawa, *J. Non - Cryst. Solids*, 10 (1988) 151.
8. K. Shimakawa, *J. Non - Cryst. Solids*, 43 (1981) 229.
9. L. Tichy and A. Triska, *Solid State Commun.*, 41 (1982) 751.
10. C. Wood , L.R. Gilbert, R. Mueller and C.M. Garner, *J. Vac. Sci. Technol.*, 10 (1973) 739.
11. H.A. Zayed, A.M. Abo - Elsoud, A.M. Ibrahim and M.A. Kenawy, *Thin Solid Films*, 247 (1994) 94.
12. H.A. Zayed, A.M. Abo - Elsoud, B.A. Mansour and A.M. Ibrahim, *Ind. J. Pure and Appl. Phys.*, 32 (1994) 334.

13. K.Y. Rajpure, U.L. Shinde and C.H. Bhosale, Natl. Conf. on energing trends in Elect. mwtt. and Eight Natl. Conven. of Electrochemists, Abstracts (1998), Jan. 28 - 30; 13 (A).
14. A.S.T.M. diffraction data file card No. 15 - 861.
15. G.P. Voutsas, A.G. Papazoglou and P.J. Rentzperis, Z. Kristallograp., 17 (1985) 261.
16. K.Y. Rajpure, C.D. Lokhande and C.H. Bhosale, Mater. Res. Bull., Vol. 34, No. 7, (1999) .
17. S.L. Ruby, L.R. Gilbert and C. Wood, Phys. Lett. A, 37 (1971) 453.
18. P. Pramanik and R.N. Bhattacharya, J. Solid State Chem., 44 (1982) 425.
19. A.K. Sharma and B. Singh, Ind. J. Pure and Appl. Phys., 23 (1985) 84.